International Journal of Engineering

Journal Homepage: www.ije.ir

Energy Absorption Analysis and Multi-objective Optimization of Tri-layer Cups Subjected to Quasi-static Axial Compressive Loading

M. A. Ghasemabadian, M. Kadkhodayan*

Department of Mechanical Engineering, Ferdowsi University of Mashhad, Mashhad, Iran

P A P E R I N F O	A B S T R A C T
	In this paper, the energy absorption features of tri-layer explosive-welded deep-drawn cups subjected to quasi-static axial compressive loading are investigated numerically and experimentally. To produce the cups, tri-layer blanks composed of aluminum and stainless steel alloys were fabricated by an explosive-welding process and formed by a deep drawing setup. The quasi-static tests were carried out at a rate of 2 mm/min. Based on the structure of the tri-layer cups and to calculate the energy absorption features of these structures, a numerical model was established and validated by experimental findings. Moreover, based on a surrogate model and using non-domain sorting genetic algorithm II, multi-objective optimizations were performed on specific energy absorption and initial peak load. The results indicated that the total absorbed energy and mean crush force of the pure stainless steel tri-layer cup were about 5.8 and 5.7 times the values of those for the pure aluminum specimen, respectively.

NOMENCLATURE

E_{abs}	Total energy absorption (J)	CFE	Crush force efficiency (CFE)
d	Crushing displacement (m)	S_E	Crush efficiency
$F(x)$	Instantaneous axial crush load (N)	δ	Maximum shortening (m)
SEA	Specific energy absorption (J/kg)	L	Original length of the structure (m)
m	Mass (kg)	T_E	Total efficiency
F_{mean}	Mean of crush force (N)	T_E^*	Specific total efficiency
$\hat{y}(\chi)$	Response vector	SEF_{mean}	the standard error for the mean crush force
χ	Vector of design variables	V	validation metri
$RMSE$	root mean square error	RDP_{Ref}	relative percentage difference

1. INTRODUCTION

Thin-walled structures are widely used for energy absorption applications due to their properties, including but not limited to, high specific energy absorption capacity, low cost, high manufacturability. Thin-walled tubes, as a well-known energy absorption structures, exhibit brilliant characteristics such as availability, low manufacturing cost, high stiffness and strength, excellent loading–carrying efficiency, excellent energy absorption efficiency and absorption of energy in a controlled manner [1-2]. Despite all the described advantages,

subjecting to axial impact loadings, these tubes show an extremely high initial peak force, which increases the possibility of serious human fatalities and injuries. To mitigate the adverse effect of the initial peak force, the researchers proposed two types of methods. Shifting the initial peak load to later stages of the energy absorption process [3] and reducing the initial peak load by introducing trigger mechanisms [4], corrugation pattern [5], bitubular systems [6] and grooved patterns [7].

Hemispherical shell is a type of thin-walled structure which has been used extensively in energy dissipation application such as nuclear reactors, aircrafts and

*Corresponding Author Email: *Kadkhoda@um.ac.ir* (M. Kadkhodayan)

spacecraft owing to their lower initial peak load and excellent energy-dissipating capacity [8].

Utilizing the low initial peak load of hemispherical thin-walled shells and the superior energy absorption properties of thin-walled tubes encouraged the researchers to study the energy absorption behavior of combined shells. Tsukamoto [9] studied the impact compressive behavior of cups with multi-layered graded structures and reported that the six-layer cups possessed high energy absorption capabilities. The mechanical behavior of combined shells subjected to dynamic and quasi-static axial loadings, was investigated by Tasdemirci et al. [10]. They showed that an increase in the thickness of the cup increased the mean crash force and the specific energy absorption. Lastly, Ghasemabadian et al. [11] considered crashworthiness characteristics to study the effect of material and geometric factors on the energy absorption behavior of bi- and single-layer cups under quasi-static axial compressive loads, experimentally. Based on their results, the layering sequence had an important influence on the energy absorption features so that cups with a stainless steel outer layer exhibited mean crush force 14% more than that of structures with the aluminum outer layer.

From the literature survey summarized above, it is evident that the researches have rarely concentrated on the energy absorption response of tri-layer cup structures. Additionally, information on the energy absorption features of such unique energy dissipation structures is very circumscribed. Correspondingly, the focus of this paper is to assess the energy absorption characteristics of tri-layer cups when subjected to quasi-static axial compressive loading. Optimization of specific energy absorption and the initial peak load of tri-layer cups, based on their thickness gradient parameter is also the original contribution from this investigation and presented within this manuscript.

2. MATERIALS AND METHODS

2. 1. Materials and Preparation Process
In this study, commercially available 304L stainless steel and 1050 aluminum plates with nominal thicknesses of 1 mm and 0.5 mm and dimensions of 0.75*1 m^2 were used. The explosive welding process was utilized to fabricate the multi-layer plates. The circular blanks of 140 mm diameter were cut by a laser machine technique and formed to the cup shape at a punch speed of 540 mm/min using a 60-ton hydraulic press and a die/punch/ blank-holder set (which has been developed by the co-authors [12]) as shown in Figure 1(a). The features of the deep drawing apparatus are summarized in Table 1. The cup geometric schematic is shown in Figure 1(b).

2. 2. Quasi-Static Axial Compression Testing
The quasi-static axial compression tests were performed to study the energy absorption features of tri-layer deep-drawn cups. All experimental tests were conducted using a Universal Testing Machine made by the Zwick Company with a load cell having a capacity of 250 kN. During the crushing testing process, the specimens were deformed between the upper moving and lower stationary crossheads at a rate of 2 mm/min, and no further fixturing was utilized for holding the specimen.

2. 3. Numerical Modeling
To better understand the deformation behavior that leads to energy absorption and to find the optimal geometry parameters of tri-layer cups made of stainless steel and aluminum, the deep drawing process and springback phenomenon as well as the quasi-static compression were modeled using ABAQUS/Explicit. According to observed minor wrinkle imperfections in the blank after deep drawing process, the simulations were considered in full geometry. The deep drawing model consisted of die, blank holder, blank, and punch, as illustrated in Figure 2(a). The die, the punch, and the blank holder were considered as rigid bodies by 4-node 3-D elements type R3D4, while the tri-layer blank was modeled using the element type C3D8R. Moreover, a "Surface-to-Surface" contact definition was established between the layers.
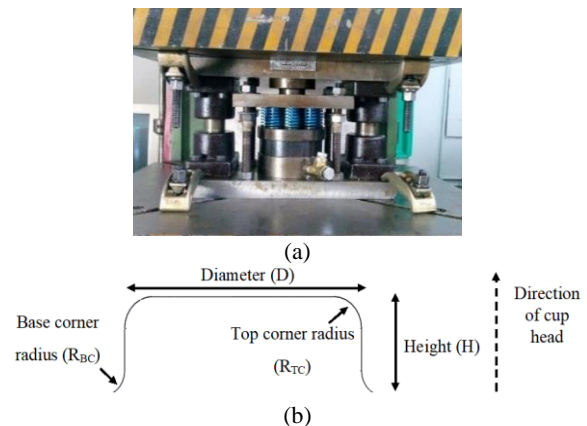

(a)

(b)

Figure 1. a) The 60-ton hydraulic press and die set, b) Schematic view of cup geometry

TABLE 1. Dimensions of deep drawing die set parts

Part	Dimension	Value (mm)
Die	Inner/ outer diameter	70/153
	Corner radius	10
Punch	Diameter	65
	Corner radius	10
Blank-holder	Inner/ outer diameter	67/167

Since the spring-back phenomenon and its residual strain and stress fields affect the accuracy of forming parts and accordingly, the quasi-static axial compression results, it is essential to predict the spring-back in the numerical modeling.

Hence, based on the state of stress and strain distribution results, the predefined field option in ABAQUS/Explicit was applied to map these fields in the quasi-static compression model. In order to observe this phenomenon caused by the deep drawing outputs, all the remaining loads, boundary conditions, and interactions of the previous simulation were eliminated and changed to new appropriate ones in the spring-back modeling.

As shown in Figure 2(b), three parts were considered in the FE model of quasi-static axial compression: the rigid bottom plate as the base, the rigid top plate as the
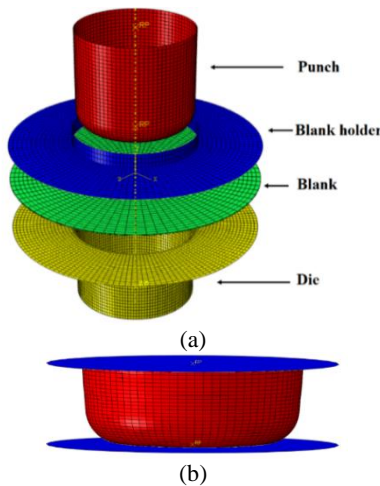

(a)

(b)

Figure 2. Finite element model a) Deep drawing, b) Crushing
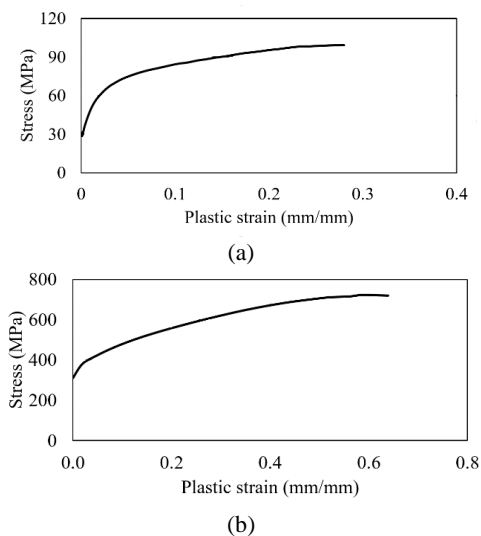

(a)

(b)

Figure 3. True stress-strain response (a) 1050 Aluminum (b) 304L stainless steel

moving plate, and the cup, which was input from the spring-back model. Furthermore, based on the mesh sensitivity study, the optimal element size of 2 mm was determined. In all models, general contact was set with the friction coefficient value of 0.3, which was obtained in previous experimental studies [10]. The contact type of "Node-to-Surface" was established between the cup edge and the base plate. The true stress-strain responses of 1050 aluminum and 304L stainless steel are represented in Figure 3.

2. 4. Specimen Grouping Information   In the current study, the modeled specimens were organized into eight types. This classification is a result of the layer order. Table 2 presents the detailed specimen grouping information, geometry dimensions, and material properties of the tri-layer cups. Each cup identified by three letters separated by forward slash (/) as "S" is for stainless steel and "A" for aluminum. Moreover, from left to right, the letters illustrate the inner, middle, and outer layers, respectively. Moreover, all of the layers were considered to have 0.5 mm thickness.

2. 5. Multi-objective Optimization Methodology
It is expected that a thin-walled energy absorber, such as a combined geometry shell, absorbs as much crash energy per unit mass as possible. Furthermore, as previously indicated [11], the initial peak load (*IPL*) is a critical load that may lead to death or severe irrecoverable injuries of occupants and should be reduced as much as possible. Hence, in the current study, maximizing specific energy absorption (*SEA*) and minimizing the initial peak load were considered as the optimization objectives.

Furthermore, two symmetric tri-layer cups, namely A/S/A and S/A/S cups having a total thickness of 1.5 mm, were considered to be optimized. The gradient parameter of κ was considered as the design parameter and defined as the ratio of the thickness of the middle layer to the total

TABLE 2. Geometric parameters and specifications of the specimens

Type	Inner layer	Middle layer	Outer layer	D	H	R_{TC}	R_{BC}
						(mm)	
S/S/S	St	St	St	65	27	10	10
S/S/A	St	St	Al	65	27	10	10
S/A/S	St	Al	St	65	27	10	10
A/S/S	Al	St	St	65	27	10	10
S/A/A	St	Al	Al	65	27	10	10
A/S/A	Al	St	Al	65	27	10	10
A/A/S	Al	Al	St	65	27	10	10
A/A/A	Al	Al	Al	65	27	10	10

thickness of the tri-layer cup, namely 1.5 mm, and was selected between 0.1 and 0.9. For example, κ=0.5 for the cup of A/S/A means that the thickness of the stainless steel layer is 0.75 mm while, the thicknesses of aluminum layers (inner and outer layers) are 0.375 mm. The deterministic multi-objective optimization problems are formulated mathematically as Equation (1):

$$\begin{cases} \max\{SEA, -IPL\} \\ s.t. \ 0.1 \le \kappa \le 0.9 \end{cases} \tag{1}$$

To calculate optimal states of the design, it is required to introduce a mathematical formulation to optimization techniques. In this study, the polynomial response surface method (PRSM) [13] was used to obtain mathematical expressions for optimization objectives, namely, *SEA* and *IPL*. In this method, an approximation $\hat{y}(\chi)$ to the structural responses is considered in terms of the simple basis functions in the form of Equation (2):

$$\hat{y}(\chi) = \sum_{j=0}^{n} a_j \varphi_j(\chi) \tag{2}$$

where $\hat{y}$ is the response vector found by numerical simulation, χ is the vector of design variables, and n is the order of polynomial function $\varphi_j(\chi)$. In the matrix form, Equation (2) may be expressed as Equation (3):

$$\hat{Y} = A\Phi \tag{3}$$

where the vector of unknown coefficients A is solved using the method of least squares as Equation (4):

$$A = (\Phi^T \Phi)^{-1}(\Phi^T y) \tag{4}$$

2. 6. Structural Crashworthiness Criteria

To study the crashworthiness performance of energy absorbers, many different criteria have been adopted, of which the following listed criteria are widely used:

Total energy absorption (E_{abs}) expressed by the Equation (5):

$$E_{abs} = \int_0^d F(x)dx \tag{5}$$

where d denotes the crushing displacement, and $F(x)$ is the instantaneous axial crush load at a distance x in the axial direction. Moreover, specific energy absorption is computed as the total energy absorption by the unit mass of the structure:

$$SEA = \frac{E_{abs}}{m} \tag{6}$$

Mean crush force (F_{mean}) is defined as the ratio of total absorbed energy to the total deformation δ:

$$F_{mean} = \frac{E_{abs}}{\delta} \tag{7}$$

Crush force efficiency (*CFE*) is expressed as the ratio of mean crush force to peak crush force as:

$$CFE = \frac{F_{mean}}{F_{max}} \tag{8}$$

The crush efficiency is obtained by the division of the maximum shortening to the original length of the structure as

$$S_E = \frac{\delta}{L} \tag{9}$$

Total efficiency is defined as the product of crush efficiency and the crush force efficiency as [14]

$$T_E = (S_E) \cdot (CFE) \tag{10}$$

Specific total efficiency (T_E^*), as the most comprehensive criterion is defined as the Equation (11):

$$T_E^* = \frac{T_E}{m} = \frac{S_E}{m} \frac{F_{mean}}{F_{max}} \tag{11}$$

3. RESULTS AND DISCUSSION

3. 1. Model Validation Assessment

To ensure that the presented FE modeling of the cups under quasi-static axial compression is sufficiently accurate, comparative studies were performed between the numerical modeling findings and the obtained experimental data. Hence, a modeled tri-layer cup with the order layer of S/A/A was compared to a two-layer explosive welded cup, which the inner layer made of stainless steel with the thickness of 0.5 mm and the outer layer made of aluminum with the thickness of 1 mm. To this end, firstly, the standard error for the mean crush force is expressed in Equation (12)

$$SEF_{mean} = \frac{(F_{mean})_N - (F_{mean})_E}{(F_{mean})_E} * 100\% \tag{12}$$

where the subscripts *N* and *E* represent the numerical and experimental values, respectively. Additionally, Oberkampf and Trucano [15] proposed the validation metric *V* as mentioned in Equation (13)

$$V = 1 - \frac{1}{L} \int_0^L \tanh\left(\left|\frac{N_{result}(\delta) - E_{result}(\delta)}{E_{result}(\delta)}\right|\right) d\delta \tag{13}$$

Moreover, the relative error is calculated as presented in Equation (14)

$$Error = \frac{1}{L} \int_0^L \left|\frac{N_{result}(\delta) - E_{result}(\delta)}{E_{result}(\delta)}\right| d\delta \tag{14}$$

The results are compared in Table 3. The results show that the values of validation metric and SEF_{mean} are 80.73 and 8.84%, respectively. Moreover, Figure 4 compares the FE and experimental results of the force/displacement responses of specimen S/A/A. It is observed that the FE findings are generally, in both qualitative and quantitative assessments, adequate in predicting experimental results. The F/D response illustrates that the initial peak force is predicted by the numerical model with a variation of 5%. Finally, the bottom views of deformed S/A/A cup from both FE modeling predictions and experimental testing are

presented in Figure 5. It is seen that the experimentally deformed cup is in good similarity to the FE results.

3. 2. Parametric Study on Energy Absorption Characteristics

In this section, based on the numerical findings, the effect of layer ordering on the energy absorption performances of tri-layer cups is discussed. The calculated energy absorption characteristics are listed in Table 4. The table was divided into three main comparisons: In the first one, the tri-layer cups made of one material were considered. In the second comparison the tri-layer cups made of one aluminum layer and two stainless steel layers were studied and in the last comparison, the cups made of one stainless steel layer and two aluminum layers were investigated. For each comparison, the shaded row is considered as the reference one within that comparison, and the parametric investigations are carried out accordingly. Furthermore, the presented relative percentage difference values (RDP), taking observations from the reference specimens, are calculated as presented in Equation (15), where R and P are the reference and the specimen observation values, respectively:

$$RDP_{Ref} = \frac{(P-R)}{R} \cdot 100\% \qquad (15)$$

TABLE 3. FE model validation assessment by Equations 12 to 14

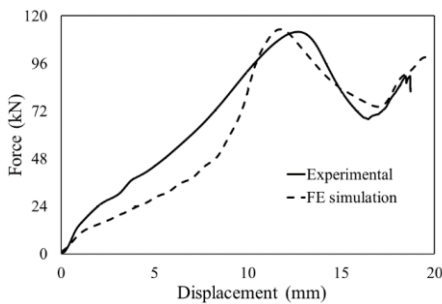| Specimen	SEF_{mean}(%)	V(%)	$Error$(%)
S/A/A	8.84	80.73	19.94

Figure 4. Force/displacement response of the cup of S/A/A
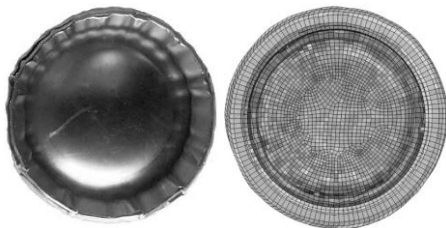

Figure 5. Comparison between bottom views of deformed S/A/A cup resulted in the experimental process and numerical modeling

TABLE 4. Numerical results of energy absorption characteristics of the tri-layer cups under quasi-static axial compression.

No.	E_{abs} (J)	F_{peak} (kN)	$SEA(\frac{kJ}{kg})$	F_{mean} (kN)	S_E	CFE	T_E	T_E^*
S/S/S	1529.7	135.8	18.28	75.62	0.749	0.557	0.417	4.98
A/A/A	264.8	24.2	9.19	13.18	0.744	0.545	0.406	14.09
S/A/S	1324.4	105.1	20.25	65.21	0.752	0.620	0.467	7.13
A/S/S	949.7	88.3	14.35	47.88	0.735	0.542	0.398	6.02
S/S/A	777.4	71.3	12.02	39.71	0.725	0.557	0.404	6.24
A/S/A	572.3	40.5	12.15	27.92	0.759	0.690	0.524	11.12
A/A/S	772.4	69.9	16.16	37.90	0.755	0.542	0.409	8.56
S/A/A	487.8	47.8	10.51	25.16	0.718	0.526	0.378	8.14

3. 2. 1. Pure Tri-Layer Cup

Energy absorption characteristics of tri-layer cups composed of one material, namely stainless steel as reference (S/S/S) and aluminum (A/A/A), are listed in Table 4. As illustrated in the table, the peak load of S/S/S specimen was observed to be approximately 5.6 times that of the A/A/A sample. Moreover, total absorbed energy and mean crush force of the pure stainless steel cup were about 5.8 and 5.7 times the values of those for the pure aluminum specimen, respectively. However, the density and consequently, the mass of stainless steel roughly three times more than those of aluminum. Hence, the absorbed energy per unit mass of S/S/S was about two times that of the aluminum specimen. Finally, the specific total efficiency of A/A/A was approximately 2.8 times that of S/S/S sample. According to the nature of specific total efficiency, it can be concluded that the pure tri-layer cup made of aluminum, is more effective in energy absorption applications than the pure stainless steel one.

3. 2. 2. Tri-Layer Cups With One Aluminum Layer

Energy absorption characteristics of tri-layer cups with one aluminum layer are listed in Table 4 and the cup with the aluminum layer as the middle layer namely, S/A/S is considered as the reference cup. Altering the layer ordering from S/A/S to S/S/A led to decrease in total energy absorption and specific energy absorption of approximately 41% and 40%, respectively while for A/S/S the changing resulted in a reduction of 28% and 29%, respectively. Moreover, changing the aluminum layer position from the middle layer to the outer layer decreased the mean crush force and peak crush force approximately of 39% and 32%, while the A/S/S cup experienced the F_{mean} and F_{max} of 26% and 16% less than those of reference cup, respectively. Furthermore, the tri-layer cup with aluminum as the inner layer illustrated total and specific total efficiencies 15% and 16%, less than those of reference cup respectively.

3. 2. 3. Tri-Layer Cups with One Stainless Steel Layer

Tri-layer cups with one stainless steel layer were considered to investigate the influence of the position of this layer on mechanical performances under quasi-static axial loading. To this end, the cup with the stainless steel as the middle layer (A/S/A) was selected as the reference configuration. Observations provided in Table 4 indicate that the change in the position from the middle layer to outer one increased the mean crush force and specific absorbed energy by approximately 36 and 33%, respectively, while total and specific total efficiencies reduced approximately 22 and 23%, respectively. Moreover, total absorbed energy and specific absorbed energy of the S/A/A were about 13 and 15% less than the values of those for the reference cup, respectively. Finally, by changing the stainless steel layer position from the middle layer to the outer and inner ones, the peak crush force increased by approximately 73 and 18%, respectively, while crush force efficiency decreased 21 and 24%, respectively.

3. 3. Optimization Findings

To find unknown coefficients of Equation (3), the sampling points of design variables were prepared from the full factorial design method. To ensure that the presented polynomial surface responses for the *IPL* and *SEA* are sufficiently accurate, the relative error (*RE*) between the numerical findings $y(\chi)$ and the approximated function $\hat{y}(\chi)$ is defined as Equation (16):

$$RE = \frac{\hat{y}(\chi) - y(\chi)}{y(\chi)} \qquad (16)$$

The root mean square error (*RMSE*) is calculated as presented in Equation (17):

$$RMSE = \sqrt{\frac{\sum_{i=1}^{n}(\hat{y}_i - y_i)^2}{n}} \qquad (17)$$

where *n* is the number of validation points. The accuracies of the PRSMs are listed in Table 5. It is evident that for the S/A/S and A/S/A cups, the RE values of the functions of *IPL* and *SEA* are less than 1%. These small errors illustrate that these PRSMs are accurate enough to perform optimization investigations. Moreover, *RMSE* values of *IPL* and *SEA* show overall accuracy of the PRSMs. In this study, to carry out the multi-objective optimization of tri-layer cups responses under quasi-static axial loading, the non-domain sorting genetic algorithm II (NSGA-II) was utilized. Figures 6 and 7 illustrate the Pareto front of multi-objective optimization of A/S/A and S/A/S cups, respectively. These Pareto fronts provide ranges of optimal solutions that can help the designers to make better decisions [16-17]. Although the Pareto fronts suggest a large number of optimal solutions to designers for the decision-making process, the final decision should be carried out based on the most satisfactory solution (termed as ''knee point'')

from the fronts. In the paper, based on the Pareto front and to define the most satisfactory solutions, the minimum distance selection method was utilized. In this method, the minimum distance between Pareto front (i.e., knee point) is introduced and an ''utopia point'' obtained using the optimal values of each individual objective. Mathematically, the method is expressed as:

$$\min D = \left[\sum_{i=1}^{m} \left(f_i^k - min(f_i) \right)^d \right]^{1/d} \qquad (18)$$

where m is the number of objective functions (m=2), f_i^k is the ith objective value in the kth Pareto solution and $d = 2, 4, 6, ...$Table 6 summarized the data of Figures 6 and 7.

Based on the given the data for optimization problem of S/A/S cup, the optimal region for *IPL* and *SEA* are [45.44 kN, 129.99 kN] and [12.20 kJ/kg, 20.82 kJ/kg], respectively, while the utopia and knee points are [20.82 kJ/kg, 45.44 kN] and [12.52 kJ/kg, 48.99 kN], respectively. In the case of A/S/A cup, the utopia value is

TABLE 5. Accuracies of the PRSMs of *IPL* and *SEA*

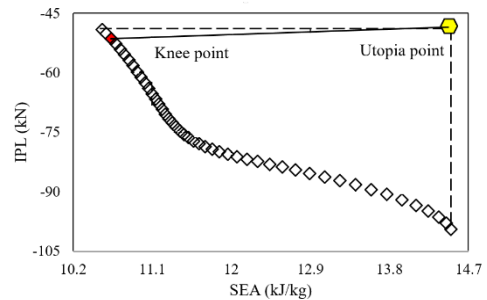| Specimen		RMSE	RE (%)
S/A/S	IPL	0.0881	[-0.268,0.171]
	SEA	0.0103	[-0.121,0.781]
A/S/A	IPL	0.4112	[-0.136, 0.153]
	SEA	0.1533	[-0.226, 0.255]

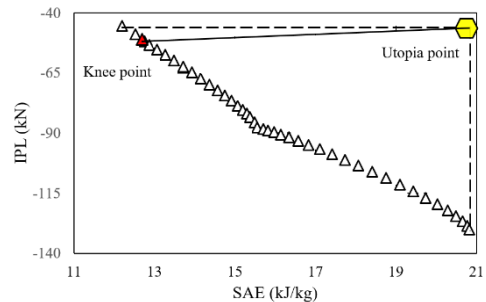**Figure 6.** Pareto front of problem of A/S/A cup

Figure 7. Pareto front of problem S/A/S cup

corresponding to specific energy absorption and the initial peak load of 14.50 kJ/kg and 49.14 kN, respectively, while the knee point occurs at the point of [10.57 kJ/kg, 51.46 kN]. Moreover, the optima region for *SEA* and *IPL* are [10.53 kJ/kg, 14.50 kJ/kg] and [49.14 kN, 99.51 kN], respectively.

To investigate the accuracy of the obtained designing schemes, comparative studies were performed out between the obtained optimization data and the numerical modeling results. To this end, the S/A/S and A/S/A cups with the dimensions corresponding to the obtained knee points were modeled numerically. The comparison results are given in Table 7.

The results show that the maximum value of relative errors of *SEA* and *IPL* for optimization and FE modeling values is 6.29%, which represents acceptable magnitudes of relative errors.

TABLE 6. Summaries of optimal designs obtained from the Pareto fronts

Optimization problem	Objective	Region	Utopia value	Knee point
S/A/S	*IPL* (kN)	[45.44, 129.99]	45.44	48.99
	SEA (kJ/kg)	[12.20, 20.82]	20.82	12.52
A/S/A	*IPL* (kN)	[49.14, 99.51]	49.14	51.46
	SEA (kJ/kg)	[10.53, 14.50]	14.50	10.57

TABLE 7. Relative errors of finite element modeling and optimization values

Optimization problem	Design parameters	Objective	Optimization results	FE modeling	Relative error (%)
S/A/S	$\kappa = 0.891$	*IPL* (kN)	48.99	47.01	4.21
		SEA (kJ/kg)	12.52	11.89	5.30
A/S/A	$\kappa = 0.446$	*IPL* (kN)	51.46	50.12	2.67
		SEA (kJ/kg)	10.57	11.28	-6.29

4. CONCLUSIONS

The current study involved experimental and numerical investigations assessing the energy absorption characteristics as well as the multi-objective optimization of tri-layer cups subjected to the quasi-static compressive axial loading. Based on the findings obtained, the following conclusions can be obtained:
1. Numerical findings illustrated that the specific total efficiency of A/A/A cup was approximately 2.8 times that of the S/S/S sample.

2. For the tri-layer cups with one stainless steel layer, it was observed that the change in the position of this layer from the middle layer to outer one increased the mean crush force, and specific absorbed energy by approximately 36% and 33%.
3. From the multi-objective optimization findings, it was observed that a tri-layer cup of A/S/A with the gradient parameter of $\kappa = 0.446$ exhibited the optimal values of *IPL* and *SEA* of 51.46 kN and 10.57 kJ/kg, respectively, while the S/A/S cup with the thickness gradient parameter of $\kappa = 0.891$ possessed the optimal values of *IPL* and *SEA* of 48.99 kN and 12.52 kJ/kg, respectively.

5. REFERENCES

1. Nateghi, F., "Improved behaviour of accordion metallic dampers affected by the increasing number of layers", *International Journal of Engineering- Transactions C: Aspects*, Vol. 28, No. 6, (2015), 864-870.

2. Maghami, S., Rezaeepazhand, J. and Yousefsani, S., "Effect of corner bluntness on energy absorbing capability of non-circular metallic tubes subjected to axial impact", *International Journal of Engineering- Transactions B: Applications*, Vol. 1025, (2013), 2495.

3. Jandaghi Shahi, V. and Marzbanrad, J., "Analytical and experimental studies on quasi-static axial crush behavior of thin-walled tailor-made aluminum tubes", *Thin-Walled Structures*, Vol. 60, (2012), 24-37.

4. Arnold, B. and Altenhof, W., "Experimental observations on the crush characteristics of aa6061 t4 and t6 structural square tubes with and without circular discontinuities", *International Journal of Crashworthiness*, Vol. 9, No. 1, (2004), 73-87

5. Sadighi, A., Eyvazian, A., Asgari, M. and Hamouda, A.M., "A novel axially half corrugated thin-walled tube for energy absorption under axial loading", *Thin-Walled Structures*, Vol. 145, (2019), 106418.

6. Azarakhsh, S., Rahi, A., Ghamarian, A. and Motamedi, H., "Axial crushing analysis of empty and foam-filled brass bitubular cylinder tubes", *Thin-Walled Structures*, Vol. 95, (2015), 60-72

7. Alavi Nia, A., Rahpeima, R., Chahardoli, S. and Nateghi, I., "Evaluation of the effect of inner and outer transverse and longitudinal grooves on energy absorption characteristics of cylindrical thin-walled tubes under quasi-static axial load", *International Journal of Crashworthiness*, Vol. 24, No. 1, (2017), 1-12.

8. Shariati, M. and Allahbakhsh, H., "Numerical and experimental investigations on the buckling of steel semi-spherical shells under various loadings", *Thin-Walled Structures*, Vol. 48, No. 8, (2010), 620-628

9. Tsukamoto, H., "Impact compressive behavior of deep-drawn cups consisting of aluminum/duralumin multi-layered graded structures", *Materials Science and Engineering: B*, Vol. 198, (2015), 25-34

10. Tasdemirci, A., Sahin, S., Kara, A. and Turan, K., "Crushing and energy absorption characteristics of combined geometry shells at quasi-static and dynamic strain rates: Experimental and numerical study", *Thin-Walled Structures*, Vol. 86, (2015), 83-93

11. Ghasemabadian, M., Kadkhodayan, M., Altenhof, W., Bondy, M. and Magliaro, J., "An experimental study on the energy absorption characteristics of single-and bi-layer cups under quasi-

static loading", *International Journal of Crashworthiness*, Vol. 24, No. 3, (2018), 272-285

12. Rajabi, A. and Kadkhodayan, M., "An investigation into the deep drawing of fiber-metal laminates based on glass fiber reinforced polypropylene", *International Journal of Engineering-Transactions C: Aspects*, Vol. 27, No. 3, (2013), 349-358.

13. Safikhani, H. and Jamalinasab, M., "Pareto optimization of two-element wing models with morphing flap using computational fluid dynamics, grouped method of data handling artificial neural networks and genetic algorithms", *International Journal of Engineering- Transactions A: Basics*, Vol. 31, (2018), 666-672.

14. Hanssen, A.G., Langseth, M. and Hopperstad, O.S., "Static and dynamic crushing of circular aluminium extrusions with aluminium foam filler", *International Journal of Impact Engineering*, Vol. 24, No. 5, (2000), 475-507

15. Oberkampf, W.L. and Trucano, T.G., "Verification and validation in computational fluid dynamics", *Progress in Aerospace Sciences*, Vol. 38, No. 3, (2002), 209-272

16. Baradaran, G. and Mahmoudabadi, M., "Optimal pareto parametric analysis of two dimensional steady-state heat conduction problems by mlpg method", *International Journal of Engineering- Transactions B: Applications*, Vol. 22, No. 4, (2009), 387-406.

17. Mahmoodabadi, M., Taherkhorsandi, M. and Safikhani, H., "Modeling and hybrid pareto optimization of cyclone separators using group method of data handling (gmdh) and particle swarm optimization (pso)", *International Journal of Engineering-Transactions C: Aspects*, Vol. 26, No. 9, (2012), 1089.

Persian Abstract

چکیده

در این مقاله ویژگی‌های جذب انرژی فنجان‌های سه‌لایه ساخته شده از ورق‌های جوش انفجاری شده تحت بارگذاری شبه‌استاتیک فشاری به صورت عددی و تجربی مطالعه می‌شود. برای ساخت فنجان‌ها، ورق‌های دو و سه‌لایه فولاد زنگ‌نزن و آلومینیوم توسط فرایند جوش انفجاری تولید و توسط فرایند کشش عمیق شکل داده شدند. بارگذاری شبه‌استاتیک نیز با نرخ بارگذاری ۲ میلی‌متر بر دقیقه بر آن‌ها انجام شد. برپایه‌ی ساختار فنجان سه‌لایه، یک مدل عددی برای محاسبه‌ی مشخصه‌های جذب انرژی ایجاد شده و با نتایج تجربی اعتبارسنجی شد. همچنین، با استفاده از الگوریتم ژنتیک، بهینه‌سازی چندهدفه بر روی جذب انرژی مخصوص و بار لهیدگی بیشینه انجام شد. نتایج نشان داد که جذب انرژی کل و میانگین بار لهیدگی ورق سه‌لایه‌ی فولاد زنگ‌نزن به ترتیب ۵/۸ و ۵/۷ برابر مقادیر مربوط به ورق سه‌لایه‌ی آلومینیوم بود.